Errors in paleomagnetism: Structural control on overlapped vectors - mathematical models.

A. Rodríguez-Pintó, M.J. Ramón, B. Oliva-Urcia, E.L. Pueyo, A. Pocoví

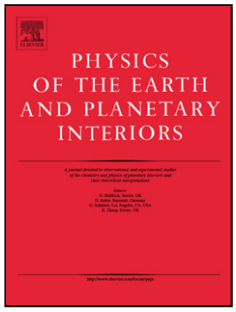

Title: Errors in paleomagnetism: Structural control on overlapped vectors - mathematical models.

Authors: A. Rodríguez-Pintó, M.J. Ramón, B. Oliva-Urcia, E.L. Pueyo, A. Pocoví

PII: S0031-9201(11)00028-8
DOI: doi:10.1016/j.pepi.2011.02.003
Reference: PEPI 5379

To appear in: *Physics of the Earth and Planetary Interiors*

Received date: 7-6-2010
Revised date: 3-2-2011
Accepted date: 5-2-2011

Please cite this article as: Rodríguez-Pintó, A., Ramón, M.J., Oliva-Urcia, B., Pueyo, E.L., Pocoví, A., Errors in paleomagnetism: Structural control on overlapped vectors - mathematical models., *Physics of the Earth and Planetary Interiors* (2010), doi:10.1016/j.pepi.2011.02.003

Errors in paleomagnetism:
Structural control on overlapped vectors - mathematical models.

Rodríguez-Pintó, A. (1,2); Ramón, M. J. (2); Oliva-Urcia, B. (1);
Pueyo, E. L. (2); Pocoví, A. (1)
(1) Geodinámica Interna. Ciencias de la Tierra, U. de Zaragoza, Spain (adrianar@unizar.es).
(2) Oficina de Proyectos de Zaragoza. Instituto Geológico y Minero de España (unaim@igme.es).

Abstract

The reliability of paleomagnetic data is a keystone to obtain trustable kinematics interpretations. The determination of the real paleomagnetic component recorded at certain time in the geological evolution of a rock can be affected by several sources of errors: inclination shallowing, declination biases caused by incorrect restoration to the ancient field, internal deformation of rock volumes and lack of isolation of the paleomagnetic primary vector during the laboratory procedures (overlapping of components). These errors will limit or impede the validity of paleomagnetism as the only three-dimension reference. This paper presents the first systematic modeling of the effect of overlapped vectors referred to declination, inclination and stability tests taking into account the key variables: orientation of a primary and secondary (overlapped to the primary) vectors, degree of overlapping (intensity ratio of primary and secondary paleomagnetic vectors) and the fold axis orientation and dip of bedding plane. In this way, several scenarios of overlapping have been modeled in different fold geometries considering both polarities and all the variables aforementioned, allowing to calculate the deviations of the vector obtained in the laboratory (overlapped) with respect to the paleomagnetic reference (not overlapped). Observations from the models confirm that declination errors are larger than the inclination ones. In addition to the geometry factor, errors are mainly controlled by the relative magnitude of the primary respect to the secondary component (P/S ratio). We observe larger asymmetries and bigger magnitudes of errors along the fold location if the primary and secondary records have different polarities. If the primary record (declination) and the fold axis orientation are perpendicular ($\Omega = 90^{o}$), errors reach maximum magnitudes and larger asymmetries along the fold surface (different dips). The effect of overlapping in the fold and reversal tests is also qualitatively analyzed in this paper.

***Keywords**: Mathematical model, overlapped vector, primary and secondary components, fold geometry, declination and inclination errors, fold and reversal tests.*

1. Introduction

Paleomagnetism provides an independent reference frame that helps from the plate-tectonic to fold-and-thrust belt scales to understand and quantify three-dimensional deformation patterns. However, any paleomagnetic study should prove: 1) the absence of inclination shallowing (in sedimentary rocks), 2) a correct restoration to the ancient reference system in case of complex deformation patterns, 3) the absence of internal deformation and 4) a perfect isolation of paleomagnetic components in the laboratory (Van der Voo, 1990). All these causes are controlled by the geometry of deformation and will introduce errors that can seriously affect the interpretation of the data (Pueyo 2010).

Concerning the last one, the main goal of the demagnetization procedures in the laboratory is to fully isolate all paleomagnetic components (Van der Voo, 1990). The overlapping of paleomagnetic components involves large number and different nature of variables: type of magnetic carrier, grain size, relaxation time and the related unblocking temperatures and coercivities, as well as the geometry of the demagnetization spectra. If there are two or more components sharing a common temperature or coercivity window, then an overlapping of components occurs and any further analysis or interpretation of paleomagnetic data may become non-sense and will lack any reliability. Partial or total simultaneous removal of two paleomagnetic components cannot be ruled out during paleomagnetic analyses. The lack of overlapping should not be assumed and the isolation of paleomagnetic components has to be effectively demonstrated by the internal coherence of the dataset.

The study of this source of error started very early during the development of paleomagnetic methods (Kramov, 1958; Halls, 1976; Roy & Lapointe, 1978; Bailey and Halls, 1984; Schmidt, 1985; McFadden, 1977 & McFadden and McElhinny, 1988; Dinarés and McClelland, 1991) but neither a diagnostic test nor a way of filtering this error have been developed until today. Other sources of error in the stability tests have been considered such as apparent synfolding results in a fold test caused by structural complications (Tauxe & Watson, 1994; Weil and Van der Voo, 2002; Pueyo, 2010) but

the influence of inaccurately isolated primary record in the stability test have remained uncovered.

Evidences of overlapping include; unexpected inclinations and declination values, inconsistence between two polarities, curved demagnetization diagrams (partial overlapped), "S" shaped demagnetization curves (if one component include another), apparent single component diagrams (if both components are removed simultaneously), in case of total overlap (Tauxe, 2009; Fig 9.10). In summary, this source of error can strongly modify the interpretation of paleomagnetic directions, magnetochrons, vertical axis rotations and also the stability tests (fold and reversal ones).

In this paper, a systematic mathematical modeling of overlapped vectors as function of the fold geometry is developed. The final goal of the model is to quantify the declination and inclination errors for a wide range of structural locations with a methodology that can be applied to any particular structural setting. Finally, a qualitative evaluation of the influence of the declination and inclination errors in the fold and reversal test is also done.

2. Apparent single component diagrams.

The case of total overlapping is very challenging because both components are simultaneously removed and an apparent single component demagnetization diagram may result (Tauxe, 2009). Thus, additional paleomagnetic or geologic information is needed to detect possible errors.

Examples of artificial Zijderveld diagrams are here used to better understand the effect of the declination and inclination errors in overlapped paleomagnetic vectors. Four different degrees of overlapping (ratio of the magnitude of the primary component respect to the secondary component: P/S) are shown, from non overlapped on the left to a higher degree of overlapping on the right are shown in Fig. 1. The overlapping is considered in a theoretical sample with two components. The primary, secondary and overlapped components are marked with numbers in the orthogonal diagrams between the points of the demagnetization spectra: 1-2 for the secondary, 3-4 for the primary and 2-3 for the overlapped components (Fig. 1). Three different structural situations are presented to see

the effect of the fold geometry (rows). A small portion of the primary isolated vector is displayed at the end of the demagnetization spectra to see the difference with the overlapped direction. As we can observe, apparent clockwise rotations and steeper inclination result in a bed striking 45º (right hand rule) and dipping 50º SE (stereographs on the right side of Fig. 1). The opposite error trend will be detected in a bed striking 135º and dipping 50º SW (counterclockwise –CCW– and shallow inclinations) the inclination error is so large that produces a change in the polarity of the primary component. In summary, the same degree of overlapping produces opposite error trends (CW/CCW- shall/steep) depending on the structural situation, thus, the main factor controlling the magnitude of declination and inclination errors in the overlapping of two components is the fold geometry.

3. Mathematical modeling of overlapped vectors in cylindrical folds

The mathematical modeling presented in this section considers the overlapping of two paleomagnetic components in a cylindrical fold. To simplify the model, a horizontal flat bed and a primary magnetic vector (P) recorded in the rock are assumed. Later, the rock pile is folded (P_f). After a given time gap, a secondary component overprints the primary signal and both components are overlapped; the result is an intermediate component (P_{of}). All variables in the model are known, thus the declination (DEC) and inclination (INC) errors associated to the overlapped component can be calculated after bedding correction in relation to the primary one (Fig. 2). The following subsections display a succinct description of variables, procedures and basic equations (the expanded description of variables, procedures and equations can be found in Appendix 1).

3.1. Description of the variables

3.1.1. *The input variables* involved in the mathematical model (Figs. 2 and 3) are:

- A primary vector (P) defined by: declination (P_{dec}), inclination (P_{inc}), intensity | P | and the normal and reverse polarities (P_N and P_R respectively).
- A secondary and postfolding vector (S) is defined by: S_{dec} ,S_{inc}, |S| that only displays one polarity (normal).
- The P/S ratio is given by the fraction of P and S intensities and represents the degree of overlapping between the two components.
- The fold axis orientation; trend (ø) (plunge is considered to be null).

- The obliquity (Ω) is the angle between the primary declination (P_{dec}), and the fold axis trend (ø)

- The dip: Since the plunge of the fold is negligible, the degree of limb rotation is equal to the dip of the limb. Dip is zero for the non-deformed position, and 90° for vertical beds, overturned beds are, in absolute value, larger than 90°.

- The "folded vector" (P_f) is the primary component after folding and before being overlapped.

3.1.2. *The output variables*

- The overlapped folded primary vector (P_{of})

- The overlapped restored primary vector (P_o) is P_{of} after bedding correction.

- Inclination (ε_{inc}) and declination (ε_{dec}) errors are the difference between the "overlapped and restored (Po)" and the primary (reference) vector (P). $\varepsilon_{inc} = Po_{inc} - P_{inc}$ and $\varepsilon_{dec} = Po_{dec} - P_{dec}$ *respectively.* It is worth noticing that the inclination error sense depends on the polarity of the primary vector; smaller inclinations than the reference (negative values of ε_{inc}) are referred as shallowing and larger ones (positives ε_{inc}) as steepening (Fig. 3) for the normal polarity. The opposite applies for the reverse polarity.

$$\begin{array}{l} !_{P_O} = a\tan(x_{P_O}/y_{P_O}) \\ !_{P_O} = a\tan(z_{P_O}/(y_{P_O}^{\,2} + z_{P_O}^{\,2})) \end{array} \rightarrow \begin{array}{l} !_{dec} = !_{P_O} - !_P \\ !_{inc} = !_{P_O} - !_P \end{array}$$

where α and β are declination and inclination respectively and x, y, z are the Cartesian coordinates (see appendix for details).

Therefore, the main variables considered in the model to calculate the declination and inclination errors (ε_{dec} and ε_{inc}) due to the overlapping of two components are the obliquity of the fold axis with respect to the primary component (Ω), the degree of folding (dip) and the P/S ratio. Since ε_{dec} and ε_{inc} depend upon these three variables as well as the polarity of the primary component, two different sets of nomograms have been produced to quantify the errors respect to the obliquity, dip and P/S (Fig. 4a and b).

3.2. Modeling equations and nomograms

These equations allow quantifying all possible declination and inclination errors and building nomograms (Fig. 4), which help understanding the nature of these errors in relation to the fold geometry. Due to the large number of involved variables, some of them are considered constant to build the nomograms: a primary magnetic record with two perfectly antipodal vectors (P_N = 000, 45 P_R = 180, -45, Fig. 3) recorded in a horizontal bed. After folding (variable Ω and dip values) the secondary field (S = 000, 55) overprints the primary record in a certain demagnetization window (temperature or coercivity). The ratio of overlapping, controlled by the intensity ratio (P/S), remains as a discrete variable. It is worth mentioning that we are considering a total overlapping of the vectors in an undetermined unblocking spectrum, which would correspond to an apparent single component in terms of Tauxe (2009).

4. Observations from Modeling

The following examples (Figs. 4, 5 and a supplementary table on-line) better illustrate the magnitude of declination and inclination errors obtained with the mathematical model. They will be used to display the subsequent implications on the fold and reversal tests (section 5).

Example 1: Effects on the polarity in a given structural position

(Dip, obliquity (Ω) and P/S ratio are constant. Figs. 4 [a&c] and 5)

This example focuses in a constant structural position: the southwestern limb of an anticline dipping 60º in a fold axis oriented at 150º respect to the primary field. The obtained declination error (ε_{dec}) of the P_R is +53° (clockwise –CW–) while the P_N will show a ε_{dec} of – 41° (counterclockwise –CCW–). Inclination errors are +5,4° for the normal primary polarity and +42 ° for the reverse one, biasing the value of the inclination to a shallower orientation in the reverse polarity and to a stepper in the normal one.

In the particular case of the hinge of the anticline or in any horizontal series (dip= 0 and hence, it is independent of Ω) the subsequent errors are noteworthy and they explained the usual deflection of normal and reverse means in horizontal magnetostratigraphic sections affected by overlapping problems. The declination remains constant (Sdec = P dec) but the P_N acquires 5° of ε_{inc} (steeper) and the reverse acquires + 85° (shallower

because of the change of polarity). This example remarks the asymmetry of the inclination errors for both polarities. However, declination may display significant errors when Sdec ≠ Pdec (whatever the reason is). Therefore, the reversal test will be affected due to the deflection of the antipodal character of the primary information.

Example 2: Effects on different positions of the fold

(variable dip; Ω and P/S are constant. Fig. 4[a&c])

A second example shows the effect of the secondary component (S) on the reverse polarity (P_R) along different locations of a fold (e.g. Ω =30°), P/S is constant and equal to 1. The ε_{dec} is -47° and the ε_{inc} is +60.4° in the southeastern limb of an anticline (dipping 30°). In the other limb (northwestern dip= -30°), the ε_{dec} is +99° and the ε_{inc} is +22.6° respectively (example 2.a in Fig. 4[a&c]). Despite of the moderated values of obliquity and dip, errors are significant and reach up to 100° of deflection. Both locations of the fold will undergo apparent shallow inclination but with different magnitudes. Now the effect on the normal polarity (P_N) for the same fold locations (Ω = 30° and dip 30° and -30°) is considered. In the southeastern limb the ε_{dec} is +20° and the ε_{inc} is +9.2° (stepper), whereas for the northwestern limb the ε_{dec} -12° and the ε_{inc} is -4,7° (shallower). The ε_{dec} are moderate but also suggest the same effect, as the deflection caused by a conical fold.

Considering a wider range of dip values (example 2.b in Fig. 4[a&c]) helps to illustrate the potential effect of an exhaustive sampling designed for the fold test. The P_R overlaps with a secondary normal one (S_N) in a fold with Ω = 120º. The observed ε_{dec} are 24°, 0°, -134°, -139°, -132° and 6° corresponding to dip values of 30º, 0º (hinge), -30º, -60º, -90º (vertical) and -120º respectively. On the other hand, the ε_{inc} for the same dip dataset will range between 68°, 85°, -1°, -19°, -35° and -39°. In the case of P_N, the ε_{dec} are -15°, 0°, 6°, 8°, 6°, -1° and the ε_{inc} are 17°, 5°, -9°, -23°, -37° and -51°. Errors are smaller for the same structural locations if the secondary and primary polarities are the same.

Errors change asymmetrically with dip, especially when the polarity of the primary and secondary components is opposite. On the contrary, and for a given obliquity (Ω = 120°), there is a relationship between the magnitude and sense of the errors and the limb symmetry; the normal polarity component in a northeastern limb will show the minimum values of ε_{dec}, while the southern limb will display the maximum errors. The reverse

component shows the contrary effect, declination errors are smaller in the southern limb and larger in the northern one.

Example 3: Effects of the obliquity on a certain dip.
(variable Ω; dip and P/S are constant. Fig. 4[a&c] and 5)

If the primary component is reverse (P_R) and the dip= -60°, the ε_{dec} and ε_{inc} will vary depending on the obliquities. For Ω = 30°, the ε_{dec} is 107º and the ε_{inc} is -1.81º. For Ω = 60°, errors are 139º and -19,2º respectively; for Ω=120° are -139º and -19.2º; and when Ω = 150°, the ε_{inc} is -107º and the ε_{inc} is -1.81º. In all these cases, the inclination is steeper. While positive ε_{dec} affect the signal in a CW manner, negative errors affect the result in CCW way. The ε_{dec} of supplementary obliquities (i.e. 45° and 135°) are of the same magnitude but opposite sign. On contrary, the ε_{inc} corresponding to the supplementary obliquities have the same magnitude and sign. Therefore, there is a remarkable symmetry: the ε_{dec} for a given obliquity is the opposite error of the supplementary one, and the ε_{inc} is equal to the value of the antipodal obliquity (Figs. 4b and 5).

Example 4: Effects of variable P/S for different locations of a given fold
(variable P/S and dip; Ω is constant. Fig. 4b [columns I to IV], Figs. 4c and 5).

Errors will change for different P/S values (2.3, 1 and 0,43). For example, when Ω = 45º and dip = ±45 (both limbs). The ε_{dec} in one limb (dip = +45º) are apparent CW for the normal polarity (+16º, +32º, +52º respectively), and CCW for the reverse polarity (-18º, -38º, -66º). The ε_{inc} are steeper in both cases: +10º, +14º, +17º for the normal vectors, and +20º, +56º and +91º for the reverse ones. In the other fold limb (dip = -45º) the ε_{dec} are –7º, -11º, -15º for the normal component and +24º, +121º and +151º for the reverse component. The ε_{inc} are shallower -8º, -14º, -19º for the normal polarity component (gray background [columns I & II]), and –14º, -3º, +44º for the reverse polarity component(white background [columns III & IV]).

A steepening of the inclination and CW rotation values associated to one limb (dip > 0) in the reverse polarity and to the other limb (dip < 0) in the normal polarity are observed. In an opposite way, a shallower inclination and CCW rotation values appear when dip < 0 in the reverse polarity and dip > 0 in the normal one. It is worth mentioning the large error amplification in the reverse polarity for dip < 0 and any P/S ratio, the ε_{dec} range between

+24º and +121º or even +151º (P/S values between 2.3, 1 and 0,43) whereas the ε_{inc} range between –3º and +44º. In other cases, the increasing of the errors as a function of the P/S value is less remarkable but still asymmetric: see for example the ε_{dec} (Ω = 45º) of the normal polarity in both limbs. The NW limb (dip > 0) display large errors (+16º, +32º and +52º), while the SE limb (dip < 0) show smaller errors for the same P/S ratios (-7º, -11º and- 15º).

Example 5: Effects of variable P/S for different folds

(variable P/S and Ω; dip is constant. Fig. 4b [II column] and 4c)

In this case, the errors in the normal polarity for different obliquities (Ω = 0º, 45º, 90º, 135º and 180º) are considered for a fixed fold location (constant dip= +30) and in two different overlapping ratios (P/S = 0,25 and 4). The ε_{inc} have the same magnitude for a given Ω and its complementary: +1º when Ω = 0º and 180º. The ε_{inc} is +5º and +19º for Ω = 45º and 135° and the same relation occurs for the ε_{dec} but with opposite sign (±7º, ±29º for Ω = 0º and 180; and ±6º and ±38º for Ω = 45º and 135º). The largest variations of the ε_{inc} for a given dip are seen for Ω = 90º (+8º and +32º) while the ε_{dec} are null.

The information derived from these examples allows us recognizing some general rules to understand the declination and inclination errors behavior:

4.1 Relationship of the errors with the obliquity (Ω)

Declination observations

Looking at the nomograms some relationships between Ω and the errors can be established. On one hand, the ε_{dec} for a given Ω is equal to the negative error of the supplementary obliquity = 180° – Ω (the antipodal obliquity, Fig. 4b [column I, rows a&e and b&d]). Maximum values of declination error (ε_{dec} around 180°), that in turn may imply an apparent polarity change in both primary polarities, are obtained for fold axes perpendicular to the primary component (Ω = 90°) and P/S $\geq$ 1 (S intensity is equal or larger than P) (Fig. 4b [I-c and III-c]). In the case of the primary reverse polarity (P_R, R in the nomograms, Fig. 4b [III and IV columns]), for a given obliquity and a decreasing P/S ratio, the ε_{dec} are very asymmetric along the fold limbs. In contrast, the ε_{dec} for a primary normal component (P_N) display the opposite behavior in the limbs of the same fold and less pronounced asymmetry (Fig. 4).

Inclination Observations

On the other hand, the ε_{inc} for a given Ω is equal to the error derived from the supplementary obliquity. Observing both limbs of a fold, the more orthogonal the P_N and the fold axis are, the more asymmetric the errors will be. Maximum values of inclination errors (ε_{inc}) for the P_R are near 90° when dip is horizontal for every obliquity. On the contrary, the maximum inclination errors for the P_N, in realistic geometries (dip < 120°, that is: 30° overturned beds), are around 55° when the fold axis and the declination of P_N are perpendicular (Ω = 90°). Notice the symmetry of Ω = 0 and Ω = 180° errors in both limbs (and both polarities) and the asymmetry of them when Ω = 90° (Fig. 4b). Finally, as a general rule, both the declination and inclination errors are larger when the primary and secondary components have opposite polarities (Fig. 4).

4.2 Declination / inclination errors and the P/S ratio

As it was be expected, decreasing values of the P/S ratio (larger overlap) will produce larger errors (ε_{dec} and ε_{inc}) in both polarities for a given location of the fold (Figs. 4 and 5). Pure mirror symmetries with respect to the axial plane of the fold are displayed when the fold axis is parallel to P and S components (Ω = 0º and 180º Fig. 4b [a&e rows]). The largest asymmetry for the declination and inclination errors between limbs is shown when the fold axis is perpendicular to the primary record (Ω = 90º Figs. 4b [row c] and 4c).

Declination observations

When there is asymmetry of errors at both limbs (for any Ω ≠ 0º &180º Figs. 4b and 4c), the ε_{dec} are bigger with positive dip and normal polarity. This implies that larger error values may be observed in the southern limb of a fold. In contrast, for reverse polarities (Fig. 4b [III & IV]) larger values are observed with negative dips corresponding to the northern flank (Fig. 4b, III column with negative dips).

Maximum ε_{dec} (180º for both polarities) are found when obliquity is Ω=90º but only when P/S≤ 1 (S ≥ P). These maximum errors mostly affect one limb; as lower the P/S ratio, wider the dip window of apparent polarity change will be. For other obliquities (Ω = 0º, 45º, 135º and 180º) in the reverse polarity, maximum ε_{dec} of 180º are also observed in a

discrete fashion; when dip = 0 (P/S < 1) or in overturned beds. Very high declination errors (>90°) will be observed between these two extreme cases.

The normal polarity declination error has a particularity; there are points of null error for every P/S value when the Po and P vector share the same declination value. This absence of error is dependent on the obliquity and will be found, for example, when Ω = 0º or 180º and dip = 0, when Ω is 45º and 135º, dip = -128º (Fig. 4b [I]).

Inclination observations

The ε_{inc} are perfectly symmetric along the fold geometry for Ω = 0º or 180º. Its asymmetry increases when the fold axis is oblique to the P direction (Fig. 4b [II & IV]). The ε_{inc} for the normal component [II], are dominantly negative (shallowing effect), while ε_{inc} in the reverse polarities are mainly positive (shallowing because the primary is negative). Their maximum values are close to the fold hinge (dip ≈ 0) in the reverse polarities (Ω = 90º) in contrast, the normal polarity maximum errors are found for overturned locations in one limb and moderate dips (given constant Ω and P/S magnitudes).

In general, there is a significant asymmetry in the errors whatever variable is considered (Ω, dip or polarity). As can be easily deduced, the overlap of components has strong influences in the stability tests.

5. The effects of the overlapping on the paleomagnetic stability tests

Non-resolved paleomagnetic components in the laboratory may induce significant changes on the stability tests, and therefore may change any geodynamic or tectonic implication of the data. In this section the general observations about the effect of overlapped directions in the fold and reversal tests are extracted by analyzing the examples previously exposed. The expected fold test result, in a non-overlapped primary component, is a significant prefolding direction and an exact antiparallel result in the reversal test. Therefore any deviation from these results will be due to the effects of the overlapping of paleomagnetic components.

5.1. Fold test

Overlapping of paleomagnetic components will turn an original primary component (prefolding with significant best-grouping at 100% unfolding), into any other possible result: significant synfolding, significant postfolding or non-significant result. The amount of departure from the expected result is basically controlled by the P/S ratio and the polarities of the primary and secondary components, although the remaining variables (obliquity, dip, etc…) have some influence in the statistical parameters as well.

Example one (Fig. 6) represents a horizontal bed followed by a monocline ($\Omega = 150°$, dip between 0º [horizontal], and 60° and P/S = 1). The overlapping of a primary component of normal polarity with a secondary component of normal polarity will generate an apparent and significant synfolding acquisition (50% unfolding). A different fold obliquity respect to the secondary direction, does not significantly change the synfolding result (Example 2; $\Omega = 30°$, dip between -30 and 30° and P/S:1, best grouping at 50%), but in this case, the synfolding character is better constrained (k values are much higher in the McElhinny test [1964]). Bootstraping (Tauxe and Watson, 1994) would inform about a postfolding normal polarity component and a non-significant record for the reverse one, although this is partially influenced by the small number of points (just two sites). In case of a tighter fold ($\Omega = 45°$ and P/S:1; example 2b) and more sites (6 different structural locations; dip from, 30 to -120 [30° overturned]) both fold tests confirm a syntectonic age of acquisition (50%) for the normal component and a non-significant result for the reverse one.

As expected, an increasing value of the intensity of the secondary direction (decreasing P/S value) will imply a gradual change from syn-tectonic to post-tectonic (example 4, Fig. 6). It is worth mentioning that, in the case of small number of samples, the McElhinny's fold test gives a more sensitive result (larger P/S implies a larger % of unfolding) than the Tauxe & Watson's (1994) one, where the larger overlapping ratios trend to show significant postfolding (instead of synfolding) directions.

Since the departure from the expected primary orientation is much larger, the fold test will be non-significant when the secondary vector has the opposite polarity than the primary one; this happens in all of the exposed examples where the degree of grouping is very little for the reverse components. All exposed examples display non-significant

results both in the McElhinny (1964), and in the Tauxe and Watson (1994), except for example 4. Here the bootstrapping for the reverse component in a given structural position (equal Ω and dip) and different P/S ratios gives non-significant result for the lowest overlapping (P/S: 2.3) and postfolding and significant for the other considered ratios (0.43 and 1).

5.2. Reversal test

Considering a similar overlapping ratio between the P and S components, the reversal test is strongly influenced by the structural position since the orientation of the "overlapped P" depends on Ω and the dip and substantially differs between the N and R components. The reversal test approach with the bootstrapping (Tauxe, 2009), could not be achieved in the exposed examples either because of insufficient number of samples or because the high scattering of the distributions. In any case, the stereographic scattering in all studied examples shows a large departure from the expected antipodal directions (starts in figure 6, left column).

6. Conclusions

Among the different potential sources of error in paleomagnetism, the overlapping of components can produce a large scattering of data. The scattering is basically controlled by the relationship between the primary and secondary magnitudes (P/S ratio), and the angular relationships of the paleomagnetic components respect to the fold geometry (fold axis orientation [Ω] and the dip of bedding planes). The mathematical model developed in this paper helps to calculate the declination and inclinations errors caused by the overlapping of two components with similar unblocking spectra during the laboratory procedure. The results of the model help establishing some general observations: (1) all errors will increase for decreasing values of the P/S magnitude (larger overlapping degree). (2) Larger errors are found if the primary direction has an opposite polarity than the secondary one. This can explain the usual large departure from antipodality in many non-deformed magnetostratigraphic studies.

In addition, the influence of the fold geometry on the declination and inclination errors can be also synthesized from the mathematical model in the following remarks: (3) opposite declination errors will affect opposite limbs of the folds. Besides, the increasing of the obliquity of the fold axis with respect to the primary direction will increase the

asymmetry of the declination errors among the fold limbs. (4) On contrary, inclination errors may display the same trend in both limbs of the fold (especially when $\Omega = 0$), but the fold obliquity may produce strong and complex asymmetries in this rule. (5) The inclination error range is usually smaller than the declination one. (6) Larger asymmetry and magnitude of errors along the fold are found if the primary direction has an opposite polarity than the secondary one.

The influence of the scattering of paleomagnetic data due to overlapping on the stability tests is critical. An original primary direction may turn into any other possible result of the fold test (synfolding, postfolding or non-significant). The larger the degree of overlapping (smaller P/S ratio) the closer will be the result to post folding. In most cases and due to the scattering, a non-significant solution of the fold test will be obtained. Reversal test is strongly affected. In fact, apparent synfolding magnetizations or poorly antiparallel directions should indicate the possibility of overlapping of paleomagnetic components.

The modeling procedure presented in this paper is useful to model any other particular structural setting, where variables may substantially differ, and it can be very useful to quantify declination and inclination errors as well as controlling the errors induced on the stability tests caused.

Acknowledgements: *This work was sponsored by a fellowship from the University of Zaragoza - BSCH - Fundación Carolina (ARP). Research financial support comes from the projects Pmag3Drest (CGL-2006-2289-BTE MEC, CGL2009-14214 and CGL2009-08969 MICINN) and 3DR3 & GeoPyrDatabases (*PI165/09 & *CTPP01/07* Gob. Aragón*). Stereographic projections were made using "Stereonet" program (6.3.2) by Richard Allmendinger to whom we are very grateful. Thank you very much to Miguel Garcés, Juanjo Villalaín, Ángel Carrancho and the people from the Fort Hoofdijjk for their support and the fruitful conversations about paleomagnetism. Fold tests were carried out thanks to the PmagPy software package from Lisa Tauxe (2009) and to the super IAPD from Trond H. Torsvik et al., University of Bergen. We also acknowledge Lisa Tauxe and Elisenda Costa for helping us in the use of the PmagPy software. Two anonymous reviewers and the editor (Keke Zhang) comments have helped us to improve the earlier version of the paper.*

Appendix 1. Mathematical procedure

Modeling equations

The overlapped primary vector (P_o) is the sum of the primary vector (P) and secondary (postfolding) one divided by the intensity coefficient r (the magnitude of the resultant vector). R is the rotation matrix and R' is the inverse rotation matrix; both described below (see Appendix).

$$P_O = R' \cdot (P_{folded} + S/r) = R' \cdot (R \cdot P + S/r) = P + R' \cdot S/r = P + S_{unfolded}/r$$

The error is the difference between the overlapped and the primary vector.

$Error = P_O - P \rightarrow$

Declination error: $\delta_{dec} = \delta_{P_O} - \delta_P$

Inclination error: $\delta_{inc} = \delta_{P_O} - \delta_P$

Rotation matrix:

$$R = \begin{bmatrix} \cos\delta\cos^2\delta(1-\cos\theta)+\cos\theta & \cos\delta\,sen\delta(1-\cos\theta) & sen\delta\,sen\theta \\ \cos\delta\,sen\delta(1-\cos\theta) & sen^2\delta(1-\cos\theta)+\cos\theta & -\cos\delta\,sen\theta \\ -sen\delta\,sen\theta & \cos\delta\,sen\theta & \cos\theta \end{bmatrix}$$

Where δ is the trend of the fold axis and $\theta = DLR$, is the magnitude of the rotation. The inverse rotation matrix R' is the rotation matrix shown above with the opposite magnitude of rotation: $\theta = -DLR$.

Summarizing

$$\begin{bmatrix} x_{P_O} \\ y_{P_O} \\ z_{P_O} \end{bmatrix} = \begin{bmatrix} \cos\delta_P\cos\delta_P & \cos\delta_P\,sen\delta_P & -sen\delta_P \\ sen\delta_P\cos\delta_P & sen^2\delta_P & \cos\delta_P \\ sen\delta_P & -\cos\delta_P & 0 \end{bmatrix} \begin{bmatrix} \cos\delta_S\cos\delta_S & \cos\delta_S\,sen\delta_S & sen\delta_S \\ \cos\delta\,sen\delta(1-\cos\theta) & sen^2\delta(1-\cos\theta)+\cos\theta & -\cos\delta\,sen\theta \\ -sen\delta\,sen\theta & \cos\delta\,sen\theta & \cos\theta \end{bmatrix} \begin{bmatrix} \cos\delta_S\cos\delta_S & \cos\delta_S\,sen\delta_S & sen\delta_S \\ sen\delta_S\cos\delta_S & sen^2\delta_S & -\cos\delta_S \\ -sen\delta_S & \cos\delta_S & 0 \end{bmatrix}$$

$$\begin{aligned} \delta_{P_O} &= a\tan(x_{P_O}/y_{P_O}) \\ \delta_{P_O} &= a\tan(z_{P_O}/(y_{P_O}^2 + z_{P_O}^2)) \end{aligned} \rightarrow \begin{aligned} \delta_{dec} &= \delta_{P_O} - \delta_P \\ \delta_{inc} &= \delta_{P_O} - \delta_P \end{aligned}$$

Coordinates conversion and conventions:

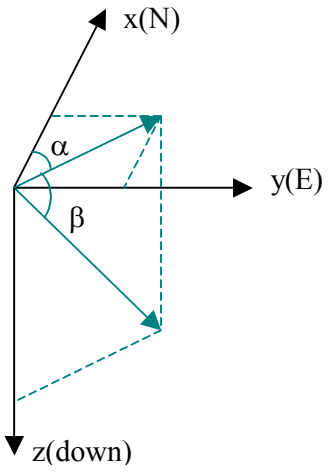

$$dec = atan(y/x)$$

$$inc = atan(z/\sqrt{x^2 + y^2})$$

$$x = \cos\delta \cos\gamma$$

$$y = sen\delta \cos\gamma$$

$$z = sen\gamma$$

530 **References**

531 Bailey, R.C. and Halls, H.C., 1984. Estimate of confidence in paleomagnetic directions
532 derived from mixed remagnetization circle and direct observational data. Journal of
533 Geophysics, 54, 174-182.
534 Dinarès-Turell, J.; McClelland, E., 1991. A cautionary tale for palaeomagnetists; a
535 spurious apparent single component remanence due to overlap of blocking-
536 temperature spectra of two components. Geophysical Research Letters. 18; 7, Pages
537 1297-1300.
538 Halls, H.C., 1976. A least-squares method to find a remanence direction from converging
539 remagnetization circles. Geophys. J.R. Astron. Sot., 45: 297-304.
540 Kramow, A. N., 1958. Paleomagnetism and stratigraphic correlation, Gostoptechizdat,
541 Leningrad. (traducción inglesa de Lojkine, A. J. y Irving, E.; Geophys. Depart.
542 Australian National University, 1960.
543 McElhinny, M.W., 1964. Statistical significance of the fold test in palaeomagnetism.
544 Geophysical Journal of the Royal Astronomical Society 8, 338–340.
545 McFadden, P. L., 1977. Comments on "A least squared method to find a remanence
546 direction from converging remagnetization circles" by H. C. Halls. Geophys. J. R.
547 Astron. Soc., 48, 549-550.
548 McFadden, P.L. and McElhinny, M.W., 1988. The combined analysis of remagnetization
549 circles and direct observations in palaeomagnetism. Earth and Planetary Science
550 Letters, 87, 161-172
551 Pueyo, E. L.; Evaluating the paleomagnetic reliability in folds and thrust belt studies.
552 Trabajos de Geologia (2011 in press)
553 Rodríguez-Pintó, A.; Ramón, M. J.; Oliva-Urcia, B.; Pueyo, E. L.; Pocoví, A.; 2010.
554 Errors in paleomagnetism: Structural control on overlapped vectors - mathematical
555 models: a case of study in the Balzes anticline (southern Pyrenees). PEPI this issue.
556 Roy, J.L. and P.L. Lapointe; 1978. Multiphase magnetizations: problems and
557 implications, Physics of the Earth and Planetary Interiors, 16 (1978) 20-37.
558 Schmidt, P.W., 1985. Bias in converging great circle methods. Earth and Planetary
559 Science Letters, 72, 427- 432.
560 Tauxe, L. & Watson, G. S. (1994). The fold test: an eigen analysis approach. Earth
561 Planet. Sci. Lett., 122, 331–341.
562 Tauxe, L., 2009. Essecials of paleomagnetism. (with contributions from: Subir K.
563 Banerjee, Robert F. Butler and Rob van der Voo).

564 Van der Voo, R., 1990. The reliability of paleomagnetic data. Tectonophysics, 184, 1-9.
565 Watson, G.S., Enkin, R.J., 1993. The fold test in paleomagnetism as a parameter
566 estimation problem. Geophysical Research Letters 20, 2135–2137.
567 Weil, A. B.; Van der Voo, R., 2002. The evolution of the paleomagnetic fold test as
568 applied to complex geologic situations, illustrated by a case study from northern
569 Spain. Physics and Chemistry of the Earth 27, 1223-1235.
570
571
572
573
574
575
576
577
578
579
580
581
582
583
584
585
586
587
588
589
590
591
592
593
594
595
596
597

598 **Figure captions**

599

600 *Figure 1: Set of artificial orthogonal plots based on different degree of overlapping (P/S*
601 *ratio and demagnetization spectra [upper row]), and different structural positions*
602 *(bedding [rows]). The P/S is assumed to be an average of the real overlapping in*
603 *the demagnetization spectrum. Columns describe demagnetization from not-*
604 *overlapped (left column)), to an important overlapped degree (right column*
605 *[P/S=1/3]), as well as intermediate situations in between (P/S = 3 and 1). Rows*
606 *describe three different structural situations: First row horizontal beds. Second row*
607 *folded beds striking 45 and dipping 50 SE. Third row folded beds striking 135 and*
608 *dipping 50 SW. The overlapped component is demagnetized between points 2 and 3*
609 *in the demagnetization spectrum. Calculated errors (ε_{dec} & ε_{inc}), are the difference*
610 *between DEC and INC of the non-overlapped vector (points 3 to 4) and the*
611 *overlapped one (2 to 3). On the right side, stereographs (lower hemisphere equal*
612 *area projection) showing the overlapped component for the different P/S ratios*
613 *together with the primary component, black (white) symbols are normal (reverse)*
614 *polarity.*

615

616 *Figure 2. Lower hemisphere stereographic projection of the parameters and variables*
617 *involved in the modeling of overlapped vectors. Left: primary, secondary and*
618 *intermediate vectors before bedding correction (BBC), (different gray-scale in*
619 *points represent vectors with intermediate overlapping degrees (Po)). Right:*
620 *Overlapped vectors after bedding correction (ABC). The difference with the*
621 *expected reference direction (non-overlapped) gives us the ε_{dec} & ε_{inc}. Observe that*
622 *inclination of P_o is shallower than the expected (inclination of P) and declination*
623 *values have an apparent counter clockwise rotation (CCW) comparing to the*
624 *reference.*

625

626 *Figure 3. Schematic 3D block diagrams and lower hemisphere stereographic projections*
627 *showing different stages of the magnetic record during folding, overlapping and*
628 *restoration of Po. The block diagrams show four stages. From left to right 1)*
629 *undeformed block, whithehead (blackhead) arrows represent reverse and normal*
630 *polarity of the primary record (P). 2) Folded position of the primary vectors. 3)*
631 *Folded and overlapped and 4) overlapped vectors restored to the horizontal. Note*

that the secondary component is assumed to be normal polarity (S_N). The solid line in the block diagrams of 1 & 2 columns represent the paleohorizontal, and dashed lines (in columns 3 &4), are the expected position of P vectors. Straight black and white arrows (3 & 4 columns, block diagram), represent the P_o vector with a P/S =1. The stereographic projections represent the four stages in both limbs of the fold to illustrate the different errors.

Figure 4. Nomograms representing the results of the mathematic model for the declination (DEC) and inclination (INC) errors (in the Y axis) against dip (in the X axis).

a) Nomograms for discrete values of the P/S ratio. Different obliquity (Ω) values as colored inner curves. Columns I and III represent the declination error for the normal and reverse polarity respectively, while columns II and IV represent the inclination errors. Negative values in the X-axis represent one limb of the fold and the positive values represent the contrary. The inner dashed boxes correspond to the enlarged area shown in Fig 4c.

b) Nomograms for discrete values of obliquity (Ω). Different P/S ratios as colored inner curves (see also Fig 4b caption).

c) Enlargement of the nomograms to better show the examples describe in the text.

Figure 5. Stereographic projection illustrating examples 1, 3 and 4 (partially). See more details in Table 1 (on-line supplementary material).

Figure 6. Fold and reversal tests. Left column represents the stereographic projection of the different examples after bedding correction. Note that they should be perfectly antipodal and they should be located at the reference direction (P) when overlapping is not present. The column in the center shows the results for the classic Mc Elhinny's (1964) fold test: evolution of the k parameter (Y axis) vs. % of unfolding (X axis). The right column shows the fold test performed with PmagPy software from Tauxe (2009).

Table 1. Data of the overlapped vectors described as examples (EX) in Figs 4&5. From left to right: EX: Number of example, Ω: Obliquity, dip: degree of limb rotation, P: polarity (Normal or Reverse), P/S: relative intensity ratio (primary/secondary), Po

DEC and Po INC: declination and inclination before bedding correction (BBC, in-situ coordinate system), So (RHR): Bedding plane orientation; azimuth, dip and dip direction following the right hand rule. Po DEC and Po INC: declination and inclination after bedding correction (ABC), ε_{dec}*: Declination error, and its sign (clockwise –CW– or counterclockwise –CCW– rotation),* ε_{inc}*: Inclination error an its effect (shallowing or steepening).*

EX	Ω	Dip	P	P/S	Po DEC	Po INC	So (RHR)			Po DEC	Po INC	Edec	effect	Einc	effect	Limb modeled	OV?
					BBC		Trend	dip	dir	ABC							
1	150	60	R	1.00	227	56	150	60	S	233	-3	53	CW	42	SHALL	SW	
	150	60	N	1.00	14	29	150	60	S	319	50	-41	CCW	5	STEEP	SW	
	150	0	R	1.00	180	40	150	0	S	180	40	0	.....	85	SHALL	.....	
	150	0	N	1.00	0	50	150	0	S	0	50	0	.....	5	STEEP	.....	
2.a	30	30	N	1.00	350	41	30	30	E	20	54	20	CW	9	STEEP	SE	
	30	30	R	1.00	138	44	30	30	E	133	15	-47	CCW	60	SHALL	SE	
	30	-30	N	1.00	18	54	210	30	S	348	40	-12	CCW	-5	SHALL	NW	
	30	-30	R	1.00	281	5	210	30	S	279	-23	99	CW	22	SHALL	NW	
2.b	120	30	N	1.00	6	37	120	30	SW	345	62	-15	CCW	17	STEEP	SW	
	120	0	N	1.00	0	50	120	0	SW	0	50	0	CW	5	STEEP	SW	
	120	-30	N	1.00	347	62	300	30	SW	6	36	6	CW	-9	SHALL	NE	
	120	-60	N	1.00	317	69	300	60	SW	8	22	8	CW	-23	SHALL	NE	
	120	-90	N	1.00	281	65	300	90	SW	6	8	6	CW	-37	SHALL	NE	
	120	-120	N	1.00	267	52	300	120	SW	359	-6	-1	CCW	-51	SHALL	NE	X
	120	30	R	1.00	201	53	120	30	NE	204	23	24	CW	68	SHALL	SW	
	120	0	R	1.00	180	40	120	0	NE	180	40	0	CW	85	SHALL	SW	
	120	-30	R	1.00	42	-17	300	30	NE	46	-46	-134	CCW	-1	STEEP	NE	
	120	-60	R	1.00	35	-4	300	60	NE	41	-64	-139	CCW	-19	STEEP	NE	
	120	-90	R	1.00	33	10	300	90	NE	48	-80	-132	CCW	-35	STEEP	NE	
	120	-120	R	1.00	33	25	300	120	NE	186	-84	6	CW	-39	STEEP	NE	X
3	30	-60	R	1.00	291	12	210	60	W	287	-47	107	CW	-2	STEEP	W	
	60	-60	R	1.00	325	-4	240	60	W	319	-64	139	CW	-19	STEEP	W	
	120	-60	R	1.00	35	-4	300	60	W	41	-64	-139	CCW	-19	STEEP	W	
	150	-60	R	1.00	69	12	330	60	W	73	-47	-107	CCW	-2	STEEP	W	
4	45	45	N	2.30	348	23	45	45	SE	16	55	16	CW	10	STEEP	SE	
	45	45	N	1.00	351	32	45	45	SE	32	59	32	CW	14	STEEP	SE	
	45	45	N	0.43	354	42	45	45	SE	52	62	52	CW	17	STEEP	SE	
	45	45	R	2.30	160	16	45	45	SE	162	-25	-18	CCW	20	SHALL	SE	
	45	45	R	1.00	147	56	45	45	SE	142	11	-38	CCW	56	SHALL	SE	
	45	45	R	0.43	34	75	45	45	SE	114	46	-66	CCW	91	SHALL	SE	
	45	-45	N	2.30	43	61	225	45	NW	353	37	-7	CCW	-8	SHALL	NW	
	45	-45	N	1.00	29	60	225	45	NW	349	31	-11	CCW	-14	SHALL	NW	
	45	-45	N	0.43	17	59	225	45	NW	345	26	-15	CCW	-19	SHALL	NW	
	45	-45	R	2.30	270	-47	225	45	NW	204	-59	24	CW	-14	STEEP	NW	
	45	-45	R	1.00	306	-4	225	45	NW	301	-48	121	CW	-3	STEEP	NW	
	45	-45	R	0.43	337	42	225	45	NW	331	-1	151	CW	44	SHALL	NW	
5	0	30	N	4.00	337	42	0	30	E	7	46	7	CW	1	STEEP	E	
	0	30	N	0.25	354	52	0	30	E	29	46	29	CW	1	STEEP	E	
	45	30	N	4.00	349	28	45	30	SE	6	50	6	CW	5	STEEP	SE	
	45	30	N	0.25	356	49	45	30	SE	38	64	38	CW	19	STEEP	SE	
	90	30	N	4.00	0	23	90	30	S	0	53	0		8	STEEP	S	
	90	30	N	0.25	0	47	90	30	S	0	77	0		32	STEEP	S	
	135	30	N	4.00	11	28	135	30	SW	354	50	-6	CCW	5	STEEP	SW	
	135	30	N	0.25	4	49	135	30	SW	322	64	-38	CCW	19	STEEP	SW	
	180	30	N	4.00	23	42	180	30	W	353	46	-7	CCW	1	STEEP	W	
	180	30	N	0.25	7	52	180	30	W	332	46	-29	CCW	1	STEEP	W